Biosensors and Bioelectronics 70 (2015) 491–497

Contents lists available at ScienceDirect

Biosensors and Bioelectronics

journal homepage: www.elsevier.com/locate/bios

Microscale electrodes integrated on COP for real sample *Campylobacter* spp. detection

M. Carmen Morant-Miñana [a,*], J. Elizalde [a,b]

[a] CIC microGUNE, Goiru kalea, 9, Polo de Innovación Garaia, 20500 Mondragón, Spain
[b] IK4-Ikerlan, P° JMª Arizmendiarrieta 2, 20500 Arrasate-Mondragón, Gipuzkoa, Spain

ARTICLE INFO

Article history:
Received 9 January 2015
Received in revised form
18 March 2015
Accepted 25 March 2015
Available online 28 March 2015

Keywords:
Electrochemical analyses
Campylobacter spp
SWV
CV
Raw meat sample

ABSTRACT

Campylobacter spp. are responsible for acute bacterial diseases in human worldwide. Nowadays campilobacteriosis is considered the most common foodborne illness in the European Union. In this paper the first electrochemical genosensor based on thin-film gold electrodes deposited onto Cyclo Olefin Polymer (COP) substrates was fabricated for the detection of *Campylobacter spp* in food matrices. The sensing element is characterized by several surface techniques and the sensitivity of the biosensor have been studied. A good linear relationship was obtained for the concentrations of PCR amplicon of *Campylobacter spp.* between 1 and 25 nM with a limit of detection (LOD) of 90 pM. Real samples have been validated with poultry meat samples and results were comparable with the PCR product samples. This is the last step for the fabrication of a Lab on a Chip (LOC), a biodevice integrating DNA sensor technology into microfluidic system, believed to perform an automated and complete assay, including sample preparation, PCR amplification, and electrochemical detection of *Campylobacter spp*. in raw poultry meat samples.

1. Introduction

Food is a relevant aspect of global public health because it plays a vital role in maintaining proper health but also causes important illness in human being. In 2010, the European Food Safety Authority (EFSA) estimated that a total of 212,064 *Campylobacter* cases in humans were reported in Europe. This represents an increase for the fifth consecutive year with 7% more cases compared to 2009 with a cost to public health systems of 2.4 billion of EUR. Several strategies have been applied for their identification and diagnosis. Mainly, classical culture media and molecular biology techniques are the traditional methods for diagnostics in foodstuffs. Campylobacter, which can cause diarrhea and fever, was mostly found in raw poultry meat. In the developing countries it is estimated that 40–60% of children under the age of 5 will develop at least one symptomatic infection, usually occurring during the first year of life and probably caused by *Campylobacter jejuni* infection (Coker et al., 2002). Isolation of *Campylobacter spp.* is difficult because the bacteria are usually present in very few numbers. For this reason, there are no commercial biosensors available to detect *Campylobacter spp* in food matrices and very few reports can be found in the literature (Yang et al., 2013).

Diagnostics are of huge importance in the healthcare system and have a critical impact on decision-making process. Currently biosensors are starting to play an interesting role in diagnostics. In particular, DNA electrochemical biosensors are faster, simpler and cheaper than traditional diagnostic methods. Thiolated DNA can be well ordered onto a gold surface by using spacer molecules between the DNA and the thiol moiety (Paleček and Bartošík, 2012). Microscale electrodes are a powerful tool for analytical chemistry and are ideally suited for their integration in miniaturized systems. They allow high current density ratios, small volumes, and the absence of supporting electrolyte, fast mass transport rates and steady-state response. They let us to measure in high resistance media such as biological fluids and food.

The advantages of these miniaturized (bio)systems include the reduction of sample and reagents volume, detection ease, minimal handling of hazardous materials and parallel multiple sample detection (Medina-Sanchez et al., 2012). To date, many reports on fabricating biomedical microdevices on solid substrates (glass, silicon and quartz) employing standard microelectronic processes have been published (Gardeniers and van den Berg, 2005). In many cases the electrodes are made of carbon or silver and are patterned on the substrate using automated screen printers (Li et al., 2012). Despite thick films are cheaper, it is well known that thin films allow the fabrication of a much more uniform and controlled resistive element giving better performance for a premium cost. Recently, Samitier et al. have reported a robust and

* Corresponding author.
E-mail address: mmorant@cicmicrogune.es (M.C. Morant-Miñana).

http://dx.doi.org/10.1016/j.bios.2015.03.063
0956-5663/

functional polymer-based sensor platform on polyethylene naphthalate (PEN) (Kuphal et al., 2012). In spite of the great results obtained in the paper, some adhesion problems were reported and a passivation layer was needed. There are other examples of analytical applications of polymer based microfluidic device (Schöning et al., 2005). Most of them are based on simple geometries that do not contain functional elements, have two electrode systems or were not tested for analytical measurements (Corgier and Juncker, 2011). In most cases polymethyl methacrylate (PMMA) is used as a prototype model. However, for market considerations PMMA presents a very fragile quality, it is easily dissolved in organic solvents and the operating temperature is limited to only 50 °C. For biological purposes other technical polymers such as COP and cyclo olefin copolymer (COC) (Niles and Coassin, 2008) can act as better polymeric platforms owing to their favorable optical properties, low impurity levels, high glass transition temperature (T_g), moldability and low water uptake (Lee et al., 2008). However, there are few reports of complete devices made of COP. Illa et al. (2010) have demonstrated the feasibility of doing aqueous and non-aqueous electrochemistry on this substrate. Using rapid prototyping techniques Abad et al. 2012 were able to successfully detect a cardiac biomarker using electrochemical measurements but the COP devices were not tested in real samples. Recently, a new COP-device involving disposable components with multiple chamber and complex microfluidic control elements was reported (Verdoy et al., 2012). The device is a complete Real-Time Polymerase Chain Reaction assay (RT-PCR) with improved sensitivity in just over 30 min. The microfluidic operation process of the device consists of the next steps: (i) clinical sample preparation, (ii) thermal cell lysis and magnetic particle target concentration and (iii) DNA amplification by real time PCR. In order to use this device as a conventional diagnosis method, the development of a new chamber for chemical or physical sensing is required.

In this paper, the biosensing component of a complete sensing microdevice applied to the detection of *Campylobacter spp.* in meat is described. The analytical method relies on the deposition of microscale thin-film based gold electrodes on COP substrates and subsequent modification of the surface with a DNA thiolated probe. The feasibility of running an electrochemical detection on PCR amplification product and meat samples is discussed based on the results obtained from atomic force microscopy (AFM), X-Ray diffraction, Fourier Transform Infrared spectroscopy (FTIR), Cyclic Voltammetry (CV) and Square Wave Voltammetry (SWV). Characterization of these electrochemical biosensors with a limit of detection (LOD) in the range of pM and in real samples is presented in detail.

2. Materials and methods

2.1. Chemicals and reagents

Tris(hydroxymethyl)aminomethane (Tris-base), ethylenediaminetetraacetic acid (EDTA), sodium hydrogen orto-phosphate, sodium dihydrogen orto-phosphate, Sodium hydroxide, acetic acid glacial, bromofenol, xylene cyanol FF, sucrose, agarose, Nancy-520, Sulphuric acid (H_2SO_4), pyrogen free water, potassium ferricyanide [K3Fe(CN)$_6$] and Mercaptohexanol were purchased from Sigma-Aldrich. Acetone 99.5% and ethanol 99.5% were supplied by Panreac. Ultra-pure water of resistivity 18.2 MΩ was obtained from a Milli-Q Water System (Millipore Corp).

2.2. Instrumentation

The CV and SWV experiments were monitored with the CH Instruments 1040B potentiostat using the EC software version at room temperature. FT-IR spectra were measured on a Perkin-Elmer Spectrum 100 spectrometer. UV/Vis spectroscopy was measured on a Biotek Eon spectrophotometer using Take3 micro-volume plate for 2 μL samples.

An Eppendorf Mastercycler personal with heated lid was used for PCR amplification. The crystallographic structure of the Au films deposited on the plastic platform was analyzed by X-ray diffraction (XRD) by means of a Philips XPERT MRD diffractometer in a glancing angle configuration (Cu Kα_1 λ=1.54059 Å). A JPK NanoWizard atomic force microscope in the intermittent contact mode using a Silicon tip with a force constant of 40 N m^{-1} and resonant frequency of approximately 300 kHz was employed to study the topography of the tested materials.

2.3. PCR primers

To detect *Campylobacter spp.* a sequence based on the flagellin gene (*flaA*) sequence (bp: 1269232–1270950) was downloaded with accession number: NC_002163.1 from Genbank in the. FASTA format. The restriction and digestion sites were simulated using the UGENE software. A fragment of 300 bp was selected and several sets of primers of ca. 25 base long were calculated using Primer-Blast (NCBI) software according to the general rules of primer design (G/C content between 50–60% and T_m of about 60 °C). Before determining the primers an alignment with BLAST program (NCBI) was performed in order to discard the primer sequence aligned with other bacteria. The primers were synthesized by Sigma-Aldrich and named as forward AAGGCGCTATGGCTGTGATGGA and reverse TGCACTCTCGGCTGCAAAGTCT.

3. Results and discussion

3.1. PCR amplification

Motility is the major factor of acute intestinal infection by Campylobacter, since non-motile variants appear unable to colonize the intestine. Campylobacter moves through the use of flagella. For this reason flagellin gens (*flaA*) have been selected as an effective way to discriminate between Campylobacter spp. with reduced swimming motility and therefore virulence. PCR amplification of Genomic DNA of *Campylobacter spp.* leads an amplicon of ca. 181 bp in approximately 1 h (see Supporting information). The fragment was moved apart by electrophoresis on a 2% agarose gel stained by Nancy-520 and visualized by UV-transilluminator. The specificity of the reaction was proven with testing different Campylobacters primers. The primers described in the literature (Ritz et al., 2009) yielded negative result and non DNA product was demonstrated showing that the primer designed are specific for campylobacter identification. The PCR was performed in different days with different concentrations of DNA. The reaction occurs in a selective way when concentrations ranging between 10 ng and 250 ng of DNA were tested. Amplifications of higher concentrations of DNA lead to unspecific product formation. PCR products were used for the hybridization with thiolated probe (ss-DNA/Au).

3.2. Sensor characterization

The election of the thermoplastic polymer COP was related to the chemical compatibility with organic solvents, low water absorption, good optical properties, excellent biocompatibility and highly resistance to acids and bases. Thin gold films of 100 nm thickness deposited on the plastic surface have a special interest for self-assembled monolayer (SAM) formation (Fig. 1). Nowadays is well-known that this formation occurs when the gold

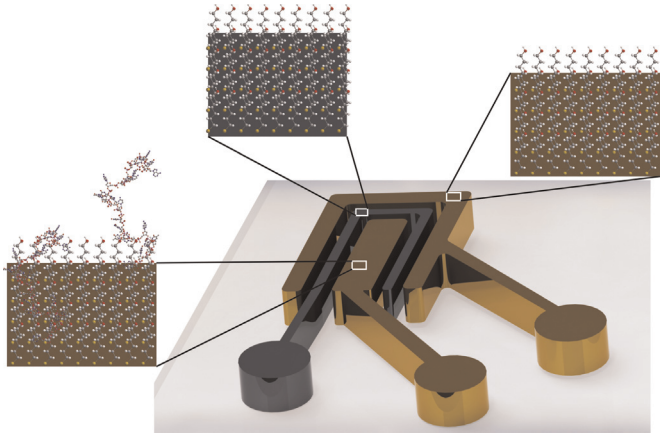

Fig. 1. Image of the electrochemical sensor with three-electrode configuration sputtered onto the COP layer.

crystallites are oriented in the (111) plane direction. Based on the fact that the substrate is crucial for the metal surface crystallization the films were studied by X-Ray diffraction to observe the orientation of the crystallites. The XRD analysis measured over squared areas of 40 mm^2 is presented in Supporting information. The position and intensity of the four diffraction peaks located at a $2\theta = 38.18°$, 44.39°, 64.57° and 77.54° match well with (111), (200), (220), (311) crystal faces of cubic Au (00-004-0784) with $a = 4.0786$Å. The patterns show that the crystallites with the (111) direction are favored. The use of glancing angle configuration ($\omega = 2°$) explains the absence of Ti reflexion (around 34.40). From the (111) diffraction peak a crystallite size of 23 nm was estimated by the Scherrer equation.

Before the measurements, the chips have been cleaned using acetone and ethanol taking into account the properties of the device. Also activation of the surface has been addressed (Carvalhal et al., 2005). The gold electrodes were electrochemically activated in sulphuric acid (0.05 M) to clean and prepare the sensor for the thiolated probe immobilization. While cleaning removes organic, inorganic and ionic species not original from the surface, activation produces a uniform metallic surface and a thin uniform oxide on the metal. A reproducible fingerprint was obtained for both independent of the type of the counter electrode. As can be observed in the Fig. 2a, both Au/Ag/Pt and Au/Ag/Au systems display a reduction peak assigned to the monolayer of oxide at ca. 0.6 V. The shape of the profile is specific to Au (111) confirming the results from XRD presented before (Hamelin, 1996).

The electrochemical surface area (ESA) calculated from the reduction peak was higher (0.047 cm^2 vs. 0.028 cm^2) in the case of the Au/Ag/Au system and can provide a better detection system. This can be attributed to the higher roughness surface calculated from several AFM images (see Supporting information). In the case of Au a higher roughness factor (2.1 nm) than Pt (1.2 nm), implies higher active surface and seems that provide a better detection. Moreover, using two electrodes made of the same metal has the advantage of diminishing the number of the steps to obtain much more cost effective chips and to increase their range of application (Zuzuarregui et al., 2015).

The stability of the system has also been evaluated to test the measurement system. The oxidation reduction peak potentials and currents were evaluated over a period of 6 weeks. After each measurement the electrodes were rinsed with water, dried under nitrogen gun and kept in at 4 °C until were measured again. The peaks remained constant during this period of time with an $E_p = 0.645 \pm 0.017$ V and $i_p = (-1.972 \pm 0.249) \times 10^{-5}$ A.

Repeatability gives us the concordance between different results measured under the same measurements conditions. The coefficient variation (%CV) was calculated as from six repeatedly prepared samples using the following equation:

$\%CV = s/x * 100$

where s is the standard deviation and x is the mean of the measurements. A value of 3.7% was obtained. Reproducibility gives us the concordance between different operators. A value of 3.5% was obtained with reproducibility conditions. For these values it can be concluded that the system is stable over a long period of time and repeatability and reproducibility requirements are acceptable with very low coefficient variations.

3.3. Detection of Campylobacter spp.

The biofunctionalization procedure of the working electrode is detailed in Supporting information. Cyclic voltammetry using ferricyanide obtained on the electrodes is showed in the Fig. 2b. Each voltammogram presents a perfect sigmoidal shape and a well-defined oxidation and reduction peaks currents corresponding to the ferro/ferricyanide redox couple. The electrochemical behavior of the electroactive $Fe(CN)_6^{3-/4-}$ redox couple is used to reflect the electron transfer characteristics of the gold surface at each modification. The anodic and cathodic peak potentials and the intensities of bare gold vs. Ag pseudo-reference electrode calculated using a mean of 8 electrodes and their standard deviation are listed in the Table 1. Using a scan rate of 0.1 V/s a formal potential ($E°$) of 0.159 V was obtained. For the bare gold voltammogram the i_{pa}/i_{pc} ratio obtained was ca. 1 and a peak potential difference ΔE_p of 0.276 V was calculated. It is interesting to note the higher ΔE value obtained compared to the one expected for a reversible process (0.059 V). This value agrees well with other values reported in the literature (Zuzuarregui et al., 2012) that integrates in a three microelectrodes system the pseudo-reference electrode and low electrolyte concentrations (Oldham, 1988). Moreover these values are obtained in the absence of supporting electrolyte which makes the system suitable for being used in low permittivity systems such as organic solvents, food or plasma (Oldham, 1992).

In electrochemical DNA hybridization sensors, a target probe of DNA is immobilized at the electrode surface. Immobilization protocols of the single strand DNA (ss-DNA) probe have been performed and tested in different sets of chips. The gold modification with a 5′ end thiolated probe of ss-DNA (via gold-thiol bond) can be detected by electrochemical measurements. The voltammograms of charged redox pairs are highly influenced by the repulsive attractive interactions with the layer that the ions must penetrate to reach the surface (Steel et al., 1998). When the electrode is modified by the thiolated probe, the penetration of the redox probe is blocked and the electron-transfer kinetics between the gold surface and the bulk solution is obstructed. As a result, a decrease of the response current and an increase in the ΔE_p (625 mV) can be observed in the voltammogram (Fig. 2b). To maintain this effect, a blocking of the electrode with 1 mM of 6-mercaptohexanol (MCH) is necessary. MCH was selected as the spacer thiol because the ss-DNA/MCH system exhibits stability, reversibility and selectivity for surface hybridization reactions (Herne and Tarlov, 1997). In absence of MCH the blocking effect is similar to that of bare gold electrode (see Supporting information). Comparison of the mixed ss-DNA probe/MCH and MCH system show that the mixed system have a higher irreversible effect (see Supporting information) as evidenced by the increased peak splitting ($\Delta p = 0.626$ V and 0.412 V, respectively). The increase of ΔE_p is due to repulsive electrostatic interactions impeding the ability of the ferricyanide anions to reach the electrode surface. These results suggest that the architecture of the monolayer consists in a densely packed layer formed by MCH and a much more dispersed layer of oligonucleotide solely immobilized though the

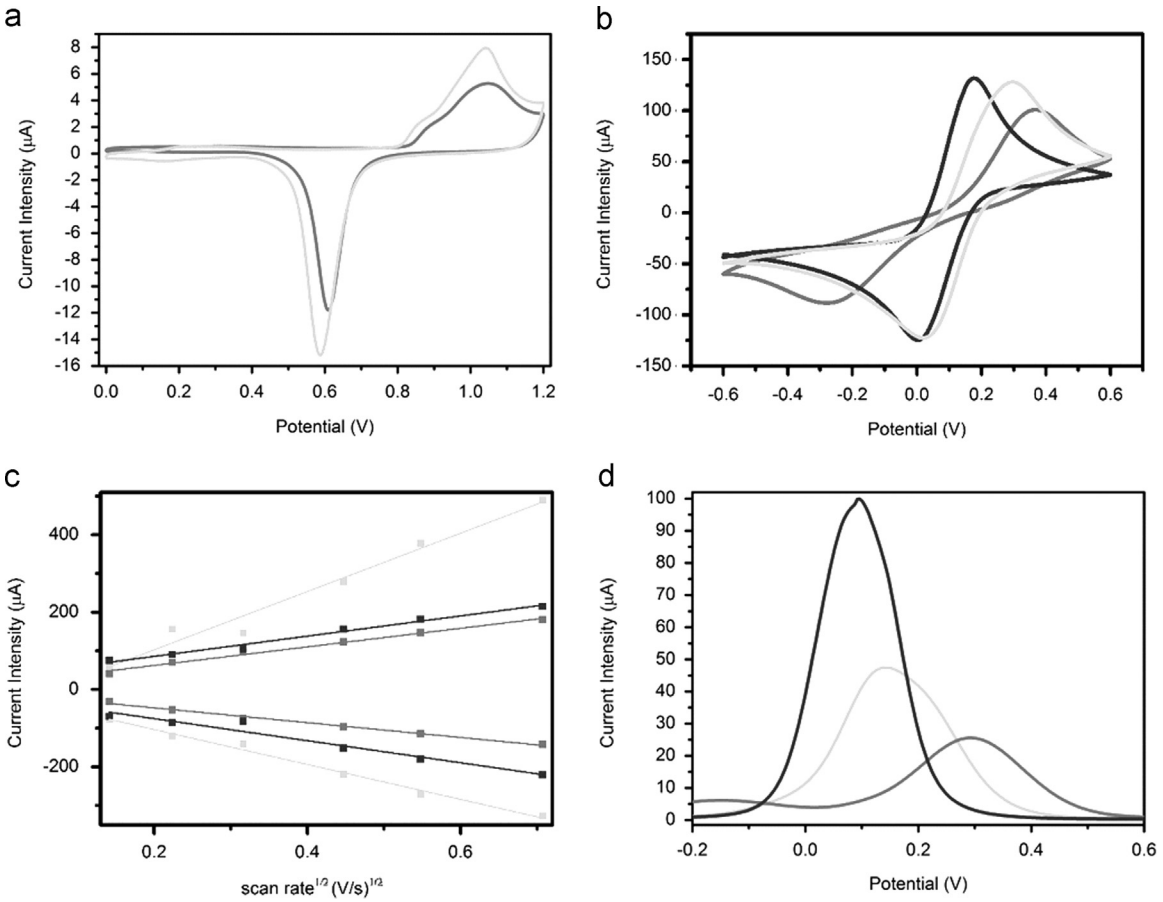

Fig. 2. Cyclic voltammograms of (a) bare gold electrodes with CE of Pt (dark gray) or Au (clear gray). (b) Bare gold electrode (clear gray), ss-DNA and MCH (dark gray) and ds-DNA (black). (c) Evolution of the current intensity with scan rate in bare gold electrode (clear gray), ss-DNA and MCH (dark gray) and ds-DNA (black). (d) Square-wave voltammograms of bare gold electrode (clear gray), ss-DNA and MCH (dark gray) and ds-DNA (black).

thiol group (Steel et al., 1998). Moreover, the MCH also acts as a blocking agent avoiding non-specific binding on the chip.

Different CV experiments have been performed after hybridation. The use of PCR product as target DNA allows for highly sensitive detection of genomic *Campylobacter spp*. The increase of oxidation peak current of ds-DNA/Au electrode (i_p=130 μA) as compared to that of the ss-DNA/Au (i_p=75 μA) can be observed clearly in Fig. 2b. The hybridization of the DNA occurs when two single stranded oligonucleotides bind via a combination of hydrogen bonding and base pair stacking. This effect favors the overlapping of the atomic orbitals with each other along the axis of DNA (Fink and Schonenberger, 1999). Since the charge transfer occurs through the DNA, it can be concluded that the increasing of the peak current is related with the hybridization of the PCR product with the ss-DNA.

The effect of the sweep rate in the peak current is observed by using the same solution and recording the CV with different scan rates from 0.02 V/s to 0.5 V/s in a potential range of −0.6 to 0.6 V. As described in the Randles–Sevcik equation, the plot of this equation yields a straight line for the oxidation and reduction peaks. The results are plotted in Fig. 2c. Both, peak intensities and separation of the peak potential ΔE_p increase with the scan rate (see Supporting information). This suggests a quasi-reversible surface electrode process of the system. The Diffusion coefficient (D) of the system can be evaluated from the slope using the value of the electroactive area (A) calculated from the oxygen reduction peak obtained in sulfuric acid aqueous solution. The magnitude of D reflects the mass transport characteristic of electroactive species diffusing to or from the electrode surface. The magnitude was calculated from either the anodic or the cathodic peak. The bare

Table 1
Electrochemical parameters measured by cyclic voltammetry.

Entry	Name	E_{pa}[a]	E_{pc}[b]	ΔE[c]	E°[d]	I_{pa}[e]	I_{pc}[f]	I_{pa}/I_{pc}	D[g]
1	BG	302 ± 3	16 ± 2	286	159	106 ± 2	−122 ± 2	0.87	(2.71 ± 2.79) × 10^{-6}
2	BI	361 ± 4	−264 ± 1	625	49	75 ± 1	−57 ± 1	1.31	(4.07 ± 1.45) × 10^{-6}
3	HY	179 ± 5	−1 ± 3	180	89	130 ± 2	−120 ± 3	1.08	(6.63 ± 0.98) × 10^{-7}

[a] Anodic peak potential (mV).
[b] E_{pc} Cathodic peak potential.
[c] ΔE (mV)=($E_{pa}-E_{pc}$).
[d] E°=($E_{pa}+E_{pc}$)/2.
[e] I_{pa}=Anodic peak Intensity (μA).
[f] I_{pc}=Cathodic peak Intensity (μA).
[g] D_0=diffusion coefficient (cm^2/s).

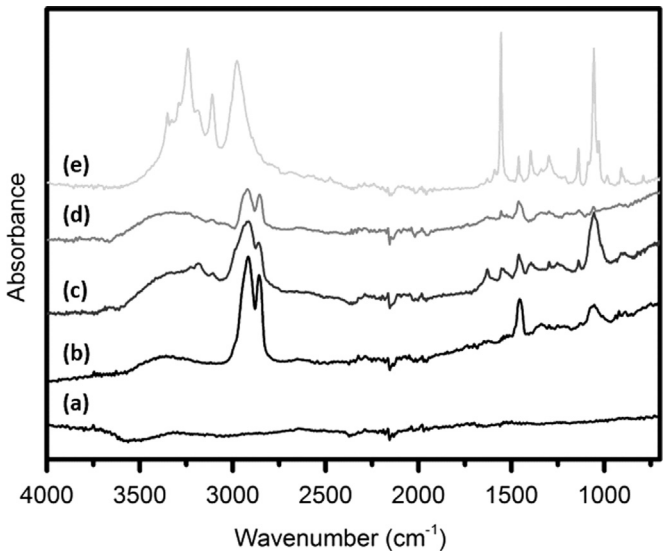

Fig. 3. FTIR spectra of the different modifications of the electrodes (a) bare gold; (b) MCH; (c) ss-DNA; (d) ss-DNA+ MCH; (e) ds-DNA (PCR product).

gold electrode give rise to D of 2.71×10^{-6} cm^2 s^{-1}, which is close to the values reported in the literature (McEwen et al., 2009). After ss-DNA immobilization, D decreases to 4.07×10^{-7} cm^2 s^{-1} because the ss-DNA/MCH layer acts as a barrier to block the diffusion of electroactive $[Fe(CN)_3]^{3-/4-}$ ions at the ss-DNA modified gold surface. When ds-DNA is achieved the obtained diffusion value is 6.63×10^{-7} cm^2 s^{-1} which is close of the double that the value of ss-DNA/MCH layer. This fact confirms that both ss-DNA/MCH are forming a compact or uniform layer on the working electrode and also the ds-DNA is acting as a wire.

The different modifications on the electrodes can be followed by FT-IR in Fig. 3. The spectrum 3a shows the transmittance of the bare gold electrode. Non-specific groups can be observed in these spectra because the surface is completely made of bare gold. After modification of the surface with the thiolated probes (Fig. 3c) in the region between 3800 and 2400 cm^{-1} the bands corresponding to –OH, –NH and –CH vibrations can be observed. Also the absorption peaks of the functional groups of the DNA can be distinguished. The peaks between 959 cm^{-1} and 1246 cm^{-1} correspond to the asymmetric and symmetric PO_4^{3-} groups of the phosphodiester deoxyribose backbone. The peaks at 1525 cm^{-1} and 1630 cm^{-1} corresponds to –NH bending and C=N stretching vibration of DNA bases of purine and pyrimidine ring (Patel et al., 2010). The peaks at 1459–1394 cm^{-1} corresponds to in plane imidazole ring vibration in adenine and guanine. The peak at 1394–1297 cm^{-1} corresponds at pyrimidine ring vibration in thymine and cytosine (Ramulu et al., 2013).

As expected, the addition of MCH results in a decrease of the characteristics functional groups of the DNA. This can be easily explained because of the lower concentration of thiolated probe (5 μM) in comparison to MCH (1 mM). Therefore, in Fig. 3d the intensities of the stretching asymmetric OH bonds are greater than those for –NH stretching and the signal corresponding to –C–OH is

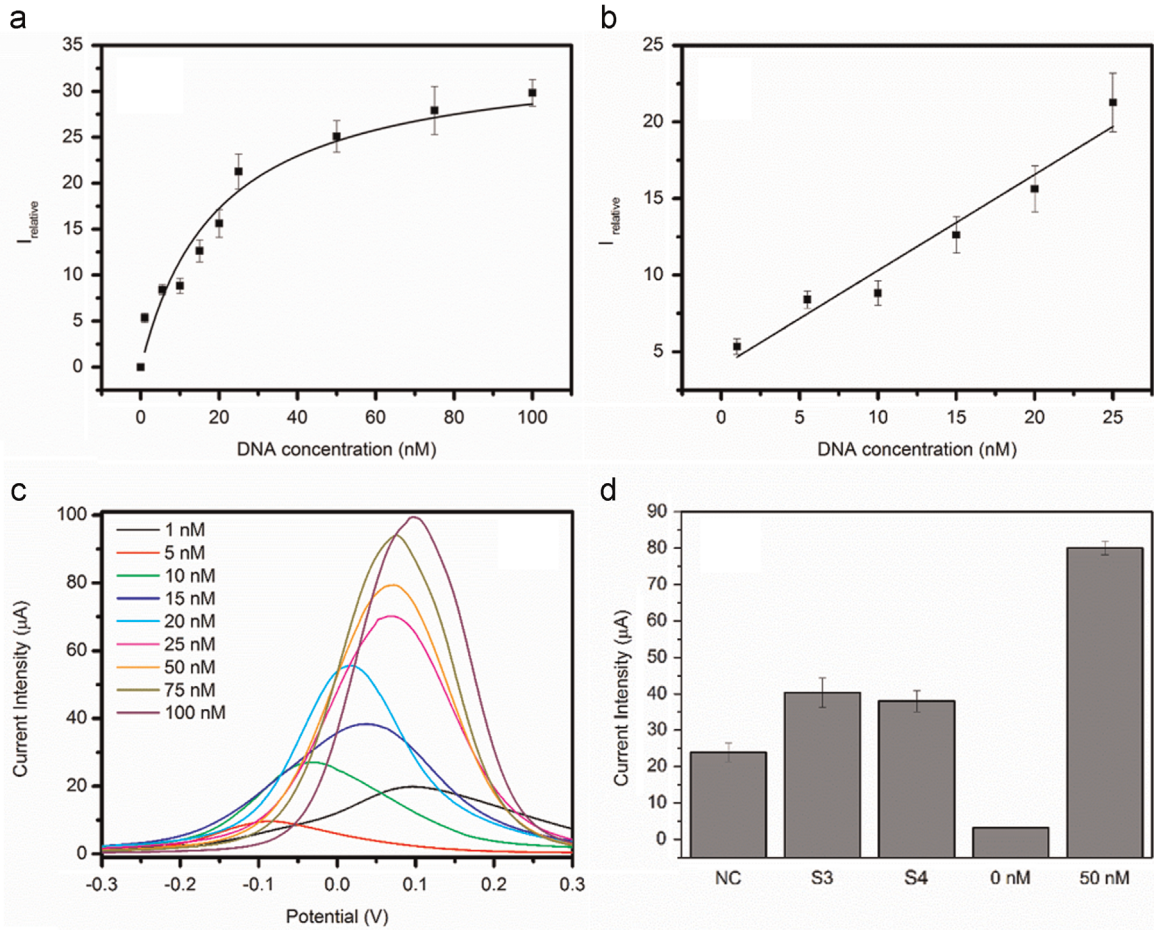

Fig. 4. (a) Hyperbolic curve between relative current intensity and increasing concentrations of PCR product of *Campylobacter spp.* (b) Lineal dependence at low PCR product concentration between 1 and 25 nM. (c) SWV hybridization response using increasing concentrations of PCR Campylobacter product. (d) Average current intensity of real sample negative control (NC) real sample 3 (S3), real sample 4 (S4), negative control from PCR product (0 nM) and 50 nM PCR product (50 nM).

also visible at 1456 cm^{-1}. After the hybridization with the PCR product (Fig. 3e) the vibration of the functional groups is restored. The complex spectral bands in the 3500–3100 cm^{-1} region correspond to the mixture of –OH and –NH vibrations. Moreover the region between 1550 and 1570 cm^{-1} is indicative of the presence of ss-DNA or ds-DNA on the gold surface. The distinction is result of the hydrogen bonds formed during base-pair formation in ds-DNA relative to ss-DNA. This hydrogen-bonding spectral region shows the ds-DNA vibration at 1557 cm^{-1} relative to the ss-DNA spectrum which is correlated with the hydrogen bond formation by the hybridization in ds-DNA that are absent in ss-DNA. This increasing in the intensity of the $–NH_2$ bending vibration are in agreement with previous reports on gold surfaces (Moses et al., 2012).

3.4. Sensitivity of the system

Square wave polarography is one of the most sensitive and direct electroanalytical techniques (Chen and Shah, 2013). The current potential waveforms obtained, being related to the first derivative of a dc polarogram, offer excellent resolution of successive electroactive species in multi-component analyses. On the basis of the results explained before the SWV obtained before and after hybridation using the three electrode system are shown in Fig. 2d. As it can be seen, hybridation of the probe with its complementary chain resulted in a dramatic enhancement of the SWV response demonstrating the high potential of this system as biosensor platform of *Campylobacter spp.* The response of the electrochemical hybridization was evaluated in the range of concentrations between 1 and 100 nM. The results are shown in Fig. 4a. The electrode monitorized with negative control does not show any change in current with a good correlation coefficient as compared to ss-DNA probe, indicating that no hybridization occurs.

To avoid variations between electrodes the normalized intensity response I_r ($I_r = I - I_0/I_0$) vs. the concentration of the PCR product was plotted. The current values, the standard deviations and the coefficient of variation obtained for each measurement are listed in Table 2. The current response of the system increases in a hyperbolic relationship with the amount of DNA from PCR product added. Three representative experiments were conducted for each concentration target. The error bars show the standard deviation ranging from 4% to 9% indicating good reproducibility of the response. A good linear relationship was obtained between 1 and 25 nM following the linear equation $I_r\,(\mu A) = 0.627\,(\mu A) + 4.033[\text{PCR-DNA}]\,(nM)$, $r = 0.977$. The sensitivity was calculated using $s = m/A$ were m is the slope of the linear equation and A is the area of the WE. The value obtained was 115.23 $\mu A/cm^2$ nM. The LOD was 90 pM calculated from $3(\sigma/m)$ where σ is the standard deviation of the blank. Quantification limit calculated as 10 (σ/m) of the blank samples was established as 0.3 nM. Recent examples of electrochemical biosensors based on SWV for different purposes have been reviewed (Chen and Shah, 2013). In food analysis applications no examples of DNA biosensors using this technique are reported. Moreover to our knowledge there are no examples of biosensors using electrochemical methods for *Campylobacter spp*. detection. Darbha et al. (2008) have developed a miniaturized gold NP-based on a Förster Resonance Energy Transfer probe for screening Campylobacter DNA with a range of detection between 0.8 and 70000 nM. No values of LOD were reported. Using diffractive optics the presence of *hip0* gene in *C. jejuni* allowed for specific detection of this pathogen with a LOD of 2.5 nM for SPR and 5 nM for the commercial kit dotLab® (Gnanaprakasa et al., 2011). Despite the high sensitivity of the optical methods in comparison to electrochemical methods similar values have been obtained in our case using electrochemical sensors.

Table 2
Current intensities, relative current intensities, standard deviations and coefficient of variation values obtained at increasing concentrations of PCR product.

Entry	Concentration	I (uA)	$(I-I_0)$/I0 (uA)	CV (%)
1	100	95.17 ± 4.64	29.83 ± 1.45	4.87
2	75	89.06 ± 8.38	27.92 ± 2.63	9.41
3	50	80.04 ± 5.44	25.09 ± 1.71	6.80
4	25	67.85 ± 6.10	21.27 ± 1.91	8.99
5	20	49.88 ± 4.84	15.64 ± 1.52	9.69
6	15	40.31 ± 3.84	12.64 ± 1.21	9.54
7	10	28.17 ± 2.6	8.83 ± 0.82	9.25
8	5	26.82 ± 1.8	8.41 ± 0.56	6.70
9	1	17.06 ± 1.6	5.35 ± 0.50	9.42
10	0	3.19 ± 0.01	–	–

The biosensor has been tested in real samples by inoculating *Campylobacter* cell in a piece of chicken. After 48 h of enrichment two samples were taken. One of the portions was scratched from the surface (S3) and the other portion was grinded in a mortar (S4). After addition of 10 ml of PBS, 0.57 g of sodium acetate, 1 ml of toluene, 5 ml of EDTA and 1 ml of SDS 10% the resulting mixture was centrifuged during 40 min at maximum speed (4400 rpm). The DNA (S3 and S4) was extracted from the supernatant using proteinase K. A portion of food was incubated without contamination as negative control (NC). The amplification yielded a band at 180 bp (see Supporting information). The amplified product was denaturalized and hybridized with the immobilization probe. After amplification the amount of *Campylobacter* was quantified using an extraction test. The values obtained were 52 nM and 54 nM for S3 and S4, respectively. The results are shown in Fig. 4d. *Campylobacter spp.* was detected in 6 of the 9 chicken samples analyzed by the biosensor. The NC samples do not have Campylobacter DNA but other compounds in the sample present a significant increase in current when the values are compared with 0 nM PCR product. For S3 and S4, the results were consistent with the sensitivity curve, although the current values obtained are lower than expected for the amount of DNA calculated. Using this genosensor the values obtained for S3 and S4 can be perfectly distinguished from the NC, confirming the positivity of the samples. The comparison of the result indicates that the DNA from real sample is being detected but the 10 times less that the DNA from PCR samples. However the working principle of the biosensor implies that the step prior of the detection is the PCR process and the whole amplification mixture is going to be transferred to the detection sample. Therefore a minimum amount of 50 nM will be introduced in all the cases in the detection chamber. Therefore the samples with current values lower that 30 μA can be considered as negative. The sensitivity of this device is similar than the reported for Manzano et al. (2015) using a fluorophore-conjugated DNA probe for meat samples diagnosis. The differences can be explained because the biosensor uses a fluorescence detection for quantitative analysis which is a more sensitive method. However higher precision, accuracy, cost effectiveness and the possibility of measure turbid samples are the main reasons for using the genosensor for *Campylobacter spp.* detection in raw meat samples.

4. Conclusions

A process to fabricate an electrochemical biosensor on polymeric substrates for selective *Campylobacter spp* detection in real food sample is described. The device is based on the deposition of thin-film gold microelectrodes which fabrication procedure is transferred directly from standard Microsystems technology. A hybrid polymer-metal system without passivation layer was easily

fabricated and characterized. The electrode surface requires electrochemical activation, which points the good performance of the device towards acids. From the biological point of view, the amplification of the bacterial genomic DNA in a short time and in a highly specific way has been done. The experimental CVs and SWVs obtained before and after hybridization suggest that the device presents a high potential to integrate electrochemistry and microfluidics for analysis of microorganism in food and therefore the samples with current values lower that 30 μA can be considered as negative.

The development of this polymer-based device is the last step for the fabrication of a microfluidic device intended to be a diagnostic tool for routine use in the food sector. To our knowledge, there no examples of this kind of devices designed for increasing the integration of functions on the chips instead of performing a single step on each device. This system complexity is required for POC diagnostics with high sensitivity and low process time compared with routine methods.

Acknowledgement

Financial support by the ETORTEK (IE13-360) program from the Ekonomiaren Garapen eta Lehiakortasun Saila (Eusko Jaurlaritza) is gratefully acknowledged.

Appendix A. Supplementary information

Supplementary data associated with this article can be found in the online version at http://dx.doi.org/10.1016/j.bios.2015.03.063.

References

Abad, Llibertat, del Campo, Francisco Javier, Muñoz, Francesc Xavier, Luis, Calavia, Daniel, Colom, Gloria, Salvador, Juan P., Marco, María Pilar, Escamilla-Gómez, Vanessa, Esteban-Fernández de Avila, Berta, Campuzano, Susana, Pedrero, María, Pingarrón, José M., Godino, Neus, Gorkin, Robert, Ducrée, Jens, 2012. Design and fabrication of a COP-based microfluidic chip: chronoamperometric detection of Troponin T. Electrophoresis 33, 3194–3287.

Carvalhal, R.F., Sanches Freire, R., Kubota, L.T., 2005. Polycrystalline gold electrodes: a comparative study of pretreatment procedures used for cleaning and thiol self-assembly monolayer formation. Electroanalysis 17 (14), 1251–1259.

Chen, A., Shah, B., 2013. Electrochemical sensing and biosensing based on square wave voltammetry. Anal. Methods 5, 2158–2173.

Coker, A.O., Isokpehi, R.D., Thomas, B.N., ko, A.;C.L.,O., 2002. Human campylobacteriosis in developing countries. Emerg. Infect. Dis. 8, 237–243.

Corgier, B.P., Juncker, D., 2011. Polymeric microfabricated electrochemical nanoprobe with addressable electrodes. Sens. Actuators B: Chem. 157 (2), 691–696.

Darbha, G.K., Lee, E., Anderson, Y.R., Fowler, P., Mitchell, K., Ray, P.C., 2008. Miniaturized sensor for microbial pathogens DNA and chemical toxins. IEEE Sens. J. 8, 693–700.

Fink, H.-W., Schonenberger, C., 1999. Electrical conduction through DNA molecules. Nature 398 (6726), 407–410.

Gardeniers, J.G.E., van den Berg, A., 2005. Microfabrication and integration - Separation methods in microanalytical systems In: Separation Methods in Microanalytical Systems. Microfabrication and Integration. Taylor & Francis, Oxford, pp. 55–106, ISBN 9780824725303.

Gnanaprakasa, T.J., Oyarzabal, O.A., Olsen, E.V., Pedrosa, V.A., Simonian, A.L., 2011. Tethered DNA scaffolds on optical sensor platforms for detection of hipO gene from *Campylobacter jejuni*. Sens. Actuators B 156, 304–311.

Hamelin, A., 1996. Cyclic voltammetry at gold single-crystal surfaces. Part 1. Behaviour at low-index faces. J. Electroanal. Chem. 407 (1–2), 1–11.

Herne, T.M., Tarlov, M.J., 1997. Characterization of DNA probes immobilized on gold surfaces. J. Am. Chem. Soc. 119 (38), 8916–8920.

Illa, X., Ordeig, O., Snakenborg, D., Romano-Rodriguez, A., Compton, R.G., Kutter, J.P., 2010. A cyclo olefin polymer microfluidic chip with integrated gold microelectrodes for aqueous and non-aqueous electrochemistry. Lab Chip 10 (10), 1254–1261.

Kuphal, M., Mills, C.A., Korri-Youssoufi, H., Samitier, J., 2012. Polymer-based technology platform for robust electrochemical sensing using gold microelectrodes. Sens. Actuators B: Chem. 161 (1), 279–284.

Lee, D.-S., Yang, H., Chung, K.-H., Pyo, H.-B., 2005. Wafer-scale fabrication of polymer-based microdevices via injection molding and photolithographic micropatterning protocols. Anal. Chem. 77 (16), 5414–5420.
Becker, H., Gartner, C., 2008. Polymer microfabrication technologies for microfluidic systems. Anal. Bioanal. Chem. 390 (1), 89–111.

Li, M., Li, Y.-T., Li, D.-W., Long, Y.-T., 2012. Recent developments and applications of screen-printed electrodes in environmental assays: a review. Anal. Chim. Acta 734 (0), 31–44.

Manzano, M., Cecchini, F., Fontanota, M., Iacumin, L., Comi, G., Melpignano, P., 2015. OLED-based DNA biochip for *Campylobacter spp.* detection in poultry meat samples. Biosens. Bioelectron. 66, 271–276.

McEwen, G.D., Chen, F., Zhou, A., 2009. Immobilization, hybridization, and oxidation of synthetic DNA on gold surface: electron transfer investigated by electrochemistry and scanning tunneling microscopy. Anal. Chim. Acta 643 (1–2), 26–37.

Medina-Sanchez, M., Miserere, S., Merkoci, A., 2012. Nanomaterials and lab-on-a-chip technologies. Lab Chip 12 (11), 1932–1943.

Moses, S., Brewer, S.H., Lowe, L.B., Lappi, S.E., Gilvey, L.B.G., Sauthier, M., Tenent, R. C., Feldheim, D.L., Franzen, S., 2004. Characterization of single- and double-stranded dna on gold surfaces. Langmuir: ACS J. Surf. Colloids 20 (25), 11134–11140.
Kumar, K.S., Naaman, R., 2012. Quantitative analysis and characterization of self-assembled DNA on a silver surface. Langmuir: ACS J. Surf. Colloids 28 (41), 14514–14517.

Niles, W.D., Coassin, P.J., 2008. Cyclic olefin polymers: innovative materials for high-density multiwell plates. Assay Drug Dev. Technol. 6, 577–590.

Oldham, K.B., 1988. Theory of microelectrode voltammetry with little electrolyte. J. Electroanal. Chem. Interfacial Electrochem. 250 (1), 1–21.

Oldham, K.B., 1992. Theory of steady-state voltammetry without supporting electrolyte. J. Electroanal. Chem. 337 (1–2), 91–126.

Paleček, E., Bartošík, M., 2012. Electrochemistry of nucleic acids. Chem. Rev. 112 (6), 3427–3481.

Patel, M.K., Solanki, P.R., Kumar, A., Khare, S., Gupta, S., Malhotra, B.D., 2010. Electrochemical DNA sensor for Neisseria meningitidis detection. Biosens. Bioelectron. 25 (12), 2586–2591.

Ramulu, T.S., Venu, R., Sinha, B., Lim, B., Jeon, S.J., Yoon, S.S., Kim, C.G., 2013. Nanowires array modified electrode for enhanced electrochemical detection of nucleic acid. Biosens. Bioelectron. 40 (1), 258–264.

Ritz, M., Garenaux, A., Berge, M., Federighi, M., 2009. Determination of rpoA as the most suitable internal control to study stress response in *C. jejuni* by RT-qPCR and application to oxidative stress. J. Microbiol. Methods 76 (2), 196–200.

Schöning, M.J., Jacobs, M., Muck, A., Knobbe, D.T., Wang, J., Chatrathi, M., Spillmann, S., 2005. Amperometric PDMS/glass capillary electrophoresis-based biosensor microchip for catechol and dopamine detection. Sens. Actuators B: Chem. 108 (1–2), 688–694.

Steel, A.B., Herne, T.M., Tarlov, M.J., 1998. Electrochemical quantitation of DNA immobilized on gold. Anal. Chem. 70 (22), 4670–4677.

Verdoy, D., Barrenetxea, Z., Berganzo, J., Agirregabiria, M., Ruano-Lopez, J.M., Marimon, J.M., Olabarria, G., 2012. A novel Real Time micro PCR based Point-of-Care device for Salmonella detection in human clinical samples. Biosens. Bioelectron. 32 (1), 259–265.

Yang, X., Kirsch, J., Simonian, A., 2013. Campylobacter spp. detection in the 21st century: a review of the recent achievements in biosensor development. J. Microbiol. Methods 95, 48–56.

Zuzuarregui, A., Morant-Minana, M.C., Perez-Lorenzo, E., Martinez de Tejada, G., Arana, S., Mujika, M., 2014. Implementation and characterization of a fully miniaturized biosensor for endotoxin detection based on electrochemical techniques. IEEE Sens. J. 14 (1), 270–277.
García, T., Revenga-Parra, Revenga-Parra, Añorga, L., Arana, S., Pariente, F., Lorenzo, E., 2012. Disposable DNA biosensor based on thin-film gold electrodes for selective Salmonella detection. Sens. Actuators B: Chem. 161 (1), 1030–1037.

Zuzuarregui, A., Souto, D., Perez-Lorenzo, E., Arizti, F., Sanchez-Gomez, S., Martinez de Tejada, G., Brandenburg, K., Arana, S., Mujika, M., 2015. Novel integrated and portable endotoxin detection system based on an electrochemical biosensor. Analyst 140, 654–660.